21

Improving the Likelihood of Success in Trials and the Efficiency of Delivery of Mucolytics and Antibiotics

Carlos F. Lange
Dept. of Mechanical Engineering, University of Alberta
Canada

1. Introduction

The use of models estimating the dosage delivered to a lung region to help design delivery systems for new drugs is well established (e.g. Finlay et al. (1997)). This approach, also called *in silico* testing, however has not yet received regulatory acceptance (Forbes et al. (2011)). A far less common application of lung deposition models is in the estimation of the concentration of the inhaled drug in the liquid layer that coats the human airways, also know as the airway surface liquid (ASL).

One case when the lung concentration of the inhaled drug is more relevant than the total deposited dosage is in the treatment of the effects of cystic fibrosis. To enhance the mucociliary clearance and to promote normal lung function in cystic fibrosis patients, mucolytic agents have been developed for aerosol delivery to the lung. These drug compounds are considered topically active, since their efficacy depends on reaching a proper concentration level, as determined by *in vitro* and *ex vivo* experiments. When designing clinical trials and treatment protocols, the total dosage delivered by inhalation needs to ensure that such concentration levels are reached in the mucus layer in each lung generation.

With the continuing emergence of multiply antibiotic-resistant organisms, the need to develop new, more powerful antibiotics remains evident. For determining an effective dose of a new antibiotic, it is common practise to use a series of clinical trials with different doses of the new drug starting from a small amount and moving to higher amounts gradually. However, resource limitations sometimes constrain the initial trial to a single dose, imposing the condition that this single attempt be effective before additional funds are made available. A requirement for efficacy of antibiotics is that the *in vivo* drug concentration be sustained at a level that ensures minimum inhibitory concentration (MIC), since otherwise resistance may be promoted.

Antibiotics and mucolytics are drugs that exhibit concentration dependence in their efficacy. Therefore, ensuring appropriate concentration of these drugs in the relevant body fluid is important for obtaining the desired therapeutic and physiological result. Until recently there had been no suitable method available to predict the amount of inhaled drug required to ensure efficacious concentration levels in the airway surface liquid (ASL).

Now, the combination of a lung deposition model with a novel model of the ASL layer allow for an estimate of the local average drug concentration in each lung generation k after inhalation

$$C_{k,\mathrm{ASL}} = \frac{m_{k,\mathrm{drug}}}{(V_{k,\mathrm{ASL}} + V_{k,\mathrm{aerosol}})} \tag{1}$$

The main focus of this chapter is to present a recently developed model that estimates local concentration of inhaled pharmaceutical aerosols in the ASL and to explain, with examples, how such a model can assist in the development of new inhaled drugs that are topically active, i.e. that depend on reaching proper concentration levels locally in the lung. Examples of recent use of this model are Desai et al. (2003); Sweeney et al. (2005); Wang et al. (2003).

2. Modelling drug deposition in the lung

To estimate the local concentration of a drug in the lung, it is necessary to estimate first the amount of drug deposited in each lung generation.

The modelling of deposition of inhaled aerosols over the years has evolved from simple and limited algebraic models (James et al. (1991)) to more complex and accurate empirical (Martonen et al. (1994)), one-way coupled (Ferron et al. (1988)), and two-way coupled hygroscopic models (Finlay & Stapleton (1995)), based on the Lagrangian approach. All these models treat the lung as unidimensional, calculating deposition on a typical or average aerosol path. While Lagrangian models can well represent the inhalation and deposition from continuous nebulizers, single breath inhalers and smart nebulizers derive their enhanced performance from time dependent effects that can only be accurately captured by Eulerian models. Eulerian deposition models have been available for many years (Egan & Nixon (1985); Roth et al. (2003); Taulbee & Yu (1975)) and recently have also incorporated one-way coupled hygroscopicity (Mitsakou et al. (2005)). However, they have not found widespread use, probably because of the relative complexity of their implementation.

The application of Computational Fluid Dynamics (CFD) to model aerosol deposition in a three-dimensional representation of the airways is relatively recent. Initially, the simulations were constrained to specific stretches of the airway path, such as the trachea and a few generations of the lung, or the alveolar region (Dailey & Ghadiali (2007)). These simulations offer some insight into the local effects of geometry on the flow, such as the tracheal rings, the shape of the carinal ridge or the size change of the alveoli. However, these analyzes are limited by the lack of upstream information about the flow.

Of all components required to predict lung deposition, arguably the most important and most challenging is the correct prediction of extrathoracic losses. These losses, compounded by inhalability losses in the case of infants and small children using masks, define the dosage actually delivered to the lung, assuming the device output is known. As DeHaan & Finlay (2001; 2004) demonstrated with dry powder inhalers, extrathoracic deposition can depart quite significantly from the baseline case of particles inhaled from a smooth, wide, straight tube with approximately constant inhalation rate studied by Stahlhofen et al. (1983). While we now understand much better the flow and deposition mechanisms occurring in the oropharyngeal region following the analysis of Heenan et al. (2004), the large scatter of data caused by intersubject variabilities even during controlled inhalation conditions (Stahlhofen et al. (1983)) would preclude any accurate prediction of extrathoracic losses. Fortunately, a comprehensive study of the effects of intersubject variability by Grgic et al.

(2004) led to the discovery of a universal form of the Stokes parameter allowing for a more accurate prediction of the oropharyngeal deposition in a wide variety of realistic mouth-throat geometries. This mathematical relationship can potentially be used to predict lung dosages from inhalers, instead of the currently used delivered dose.

One-dimensional, dynamical lung deposition models, though heavily simplified with respect to the airway geometry, can incorporate all the fundamental physical processes that affect particle size and deposition at a small fraction of the computational effort of CFD. Naturally, these 1-D models cannot resolve local deposition patterns, such as required by a tumour, but they can be properly tuned to give accurate results for delivery of drugs that target an entire lung region. The treatment of lung diseases associated with cystic fibrosis, such as bacterial infections and mucolytic treatments, are examples of cases that target a single lung region, namely the tracheobronchial region. Advanced one-dimensional models can provide this regional deposition information with high accuracy, as demonstrated by Finlay, Lange, Li & Hoskinson (2000). For these reasons, 1-D models seem better suited for the use in the modelling of local concentration of deposited drugs in the lung.

3. Modelling mucus and the Airway Surface Liquid layer

The model of the Airway Surface Liquid (ASL) layer, developed at the University of Alberta by the author in collaboration with W. Finlay and M. King (Finlay, Lange, King & Speert (2000); Hasan & Lange (2007); Lange et al. (2001)) is the first and, to this date, the only model of its kind. The model approximates the amount of liquid matter present in each lung generation, which, in conjunction with the local dosage provided by the deposition model, allows for the estimate of the local concentration of the inhaled drug.

A previous attempt to estimate concentration of deposited aerosols was performed by Böhm et al. (2003). They used an empirical estimate of lung deposition and a simple assumption of a constant thickness of the ASL layer in a single generation. An approach closer to the one proposed here was employed by Kimmel et al. (2001) to study transient clearance and mucus concentration in rats. But the mucus layer thickness was considered constant throughout the tracheobronchial region.

The ASL model distinguishes two layers with essentially different physical properties: the periciliary liquid layer (PCL), a watery layer (sol) covering the airway epithelium, and the mucus layer, a viscoelastic gel that floats on top of the PCL (see Fig. 1).

The volume of liquid in each layer is modelled separately. The sum of the two gives the total ASL volume in each generation, $V_{k,\mathrm{ASL}}$. For the calculation of the volume we assume a continuous annular layer of liquid along each generation. Figure 2 shows a schematic cross-sectional view of an airway.

The dimensions of the airways are obtained from the lung geometry model by Finlay (2001), which has been shown to correlate well with *in vivo* regional deposition experiments (Finlay, Hoskinson & Stapleton (1998)). The geometry assumes a symmetric branching airway system, starting from the extrathoracic region (mouth cavity, pharynx and larynx), followed by the trachea, and branching symmetrically into two main bronchi, then into four lobar bronchi, and so on. Each new branch segment is called a generation, k. The trachea is considered the first generation ($k = 0$), and the main bronchi are $k = 1$, so that the number of airways in each generation is always 2^k.

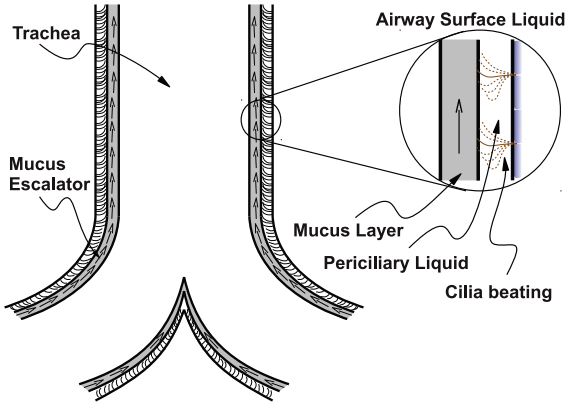

Fig. 1. Schematic of the airways with ASL layer and mucociliary escalator.

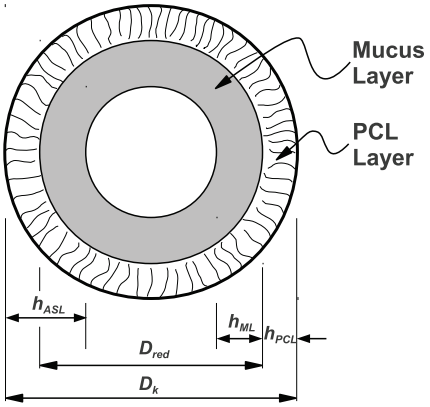

Fig. 2. Airway cross-section with PCL and mucus layers.

In contrast with the classical lung model, Weibel A (Weibel (1963)), which considers generations 0–16 to form the tracheobronchial region, Finlay's model sets the transition between the tracheobronchial region and the more distal alveolar region at the generation 14. This distinction is relevant, because mucociliary transport exists only in the conductive airways, starting at the terminal bronchioles, which are the most distal ciliated airways. While the calculation of the deposited dosage, described above, utilizes the complete lung geometry, the ASL layer is only defined in the tracheobronchial region. The dimensions of the airways in each tracheobronchial generation are reproduced from Finlay (2001) in Table 1.

The ASL model uses the same average airway diameter and length in generation k as the deposition model, D_k and L_k. With these geometric characteristics, the volume of ASL in generation k can be calculated as

$$V_{k,\mathrm{ASL}} = \pi\, L_k\, 2^k \left(D_k\, h_{k,\mathrm{ASL}} - h_{k,\mathrm{ASL}}^2 \right) \tag{2}$$

where the thickness of the ASL layer, $h_{k,\mathrm{ASL}}$, needs to be determined and is defined as

$$h_{k,\mathrm{ASL}} = h_{k,\mathrm{PCL}} + h_{k,\mathrm{ML}} \tag{3}$$

Generation	Length [cm]	Diameter [cm]
0	12.456	1.810
1	3.614	1.414
2	2.862	1.115
3	2.281	.885
4	1.780	.706
5	1.126	.565
6	.897	.454
7	.828	.364
8	.745	.286
9	.653	.218
10	.555	.162
11	.454	.121
12	.357	.092
13	.277	.073
14	.219	.061

Table 1. Airway dimensions in the tracheobronchial tree (from Finlay (2001)).

i.e., it is the sum of $h_{k,\mathrm{PCL}}$ and $h_{k,\mathrm{ML}}$, the thicknesses of the PCL and mucus layers, respectively.

In certain cases, such as in the inhalation of mucolytics, it is the volume of mucus only that is required. In this case, the same assumptions as above give

$$V_{k,\mathrm{ML}} = \pi L_k 2^k \left(D_{k,\mathrm{red}} h_{k,\mathrm{ML}} - h_{k,\mathrm{ML}}^2 \right) \tag{4}$$

where $D_{k,\mathrm{red}}$ is the airway diameter reduced by the PCL layer thickness

$$D_{k,\mathrm{red}} = D_k - 2 h_{k,\mathrm{PCL}} \tag{5}$$

Since the airway geometry follows the deposition model and is known, all that is required to estimate the volumes of mucus and ASL are the layer thicknesses. In the following sections the calculation of the PCL and mucus layer thicknesses is described.

3.1 Thickness of PCL layer

The PCL layer is formed by a watery liquid that facilitates the beating of the cilia and keeps the thicker mucus layer afloat at an exact distance to be reached by the tip of the cilia during their forward beating (Widdicombe (1997)). Although the regulation mechanism of the PCL layer thickness in the airways is still the subject of controversy (Matsui et al. (1998)), it is recognized that this regulated thickness is well approximated by the length of the cilia.

Measurements of cilia lengths in humans were performed by Serafini & Michaelson (1977) and are given in Table 2.

Two curve fits were tested to approximate the Serafini and Michaelson measurements with a smooth curve along the entire tracheobronchial region. The fitted functions that estimate the cilia length at generation k, and by extension the thickness of the PCL layer, are

$$h_{k,\mathrm{PCL}} = 5.911\, \mathrm{e}^{-k/13.4048} \qquad \text{(fit1)} \tag{6}$$

Generation	Length [μm]
0	6.03
3	4.70
5	3.87
6	3.72
7	3.60

Table 2. Human ciliary length in various lung generations from measurements.

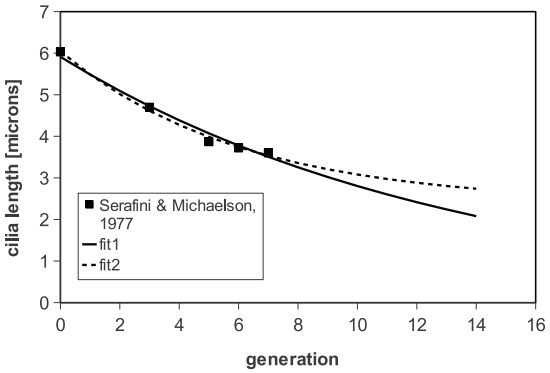

Fig. 3. Experimental and curve fitted values of cilia length in humans.

Generation	$h_{k,\mathrm{PCL}}$ [μm]
0	6.04
1	5.49
2	5.02
3	4.61
4	4.27
5	3.99
6	3.74
7	3.53
8	3.36
9	3.21
10	3.08
11	2.97
12	2.88
13	2.81
14	2.74

Table 3. Human ciliary length and PCL thickness in various lung generations.

$$h_{k,\mathrm{PCL}} = 2.3717 + 3.6724\,\mathrm{e}^{-k/6.0837} \qquad \text{(fit2)} \tag{7}$$

A plot of the raw data and of both curves can be seen in Fig. 3.

Curve fit "fit2" was selected as best fit and the corresponding values of thickness of the PCL layer, based on eq. 7 above, are shown in Table 3.

3.2 Mucus layer thickness

The mucus layer is essentially a gel formed by secretions from goblet cells located in the airway epithelium and also from submucosal glands in the larger airways (Widdicombe (1997)). The thickness of the mucus layer is estimated assuming a continuous layer of constant thickness in each generation, using mass conservation, and modelling the average mucus velocity and production rate for each generation.

The mucus layer is constantly driven by the coordinated beating of airway cilia from the distal generations to the trachea forming the so-called mucus escalator, as illustrated in Fig. 1. The 14^{th} generation is assumed to be the most distal tracheobronchial generation, as described above, where mucus production starts. In reality, as there is no sharp transition from the alveolar region to the tracheobronchial region, the mucus production also does not start always at the 14^{th} generation. In addition, in the more distal generations the mucus layer is not yet fully continuous, but there are probably patches of mucus until the cumulative production ensures full coverage of the airways. For lack of a better alternative, the present model assumes that mucus production starts at generation 14 and forms a continuous annular layer from the onset.

Mucus is actually continuously produced along the conductive airways. The amount produced at a generation k joins the cumulative amount produced at all previous (more distal) generations up to that generation, as the mucus is transported towards the trachea. The amount of mucus that flows through generation k is the accumulated amount produced up to this point, i.e. the sum of all mucus produced by generations $k+1$ to 14, plus the locally produced amount ($\dot{p}_k$). This local total production is called $\dot{P}_k$.

The flow rate of mucus through all airways of a generation is equal to the product of the annular cross-sectional area of the mucus layer, $A_{k,\mathrm{ML}}$, and the mucociliary transport velocity at this generation (clearance velocity), U_k, i.e.

$$\dot{P}_k = A_{k,\mathrm{ML}}\, U_k = 2^k\, \pi\, \left(D_{k,\mathrm{red}}\, h_{k,\mathrm{ML}} - h_{k,\mathrm{ML}}^2 \right)\, U_k \tag{8}$$

where $D_{k,\mathrm{red}}$ is defined in eq. 5, and the cumulative production rate $\dot{P}_k$ at generation k is defined by the recursive formula

$$\dot{P}_k = \dot{p}_k + \dot{P}_{k+1} \tag{9}$$

where $\dot{p}_k$ is the local production rate at generation k. The estimates of $\dot{p}_k$ are described below in section 3.3.

Equation 8 is a quadratic polynomial in terms of $h_{k,\mathrm{ML}}$

$$2^k\, \pi\, U_k\, h_{k,\mathrm{ML}}^2 - 2^k\, \pi\, U_k\, D_{k,\mathrm{red}}\, h_{k,\mathrm{ML}} + \dot{P}_k = 0 \tag{10}$$

whose only physical solution is

$$h_{k,\mathrm{ML}} = \frac{2^k\, \pi\, U_k\, D_{k,\mathrm{red}} - \sqrt{(2^k\, \pi\, U_k\, D_{k,\mathrm{red}})^2 - 4\,(2^k)\, \pi\, U_k\, \dot{P}_k}}{2\,(2^k)\, \pi\, U_k} \tag{11}$$

Rearranging the terms and defining the reduced airway radius corresponding to $R_{k,\mathrm{red}} = D_{k,\mathrm{red}}/2$, eq. 11 can be rewritten

$$h_{k,\mathrm{ML}} = R_{k,\mathrm{red}} - \sqrt{R_{k,\mathrm{red}}^2 - \frac{\dot{P}_k}{2^k \, \pi \, U_k}} \tag{12}$$

Hence, the average thickness of the mucus layer in a generation can be determined, if the cumulative production up to that generation ($\dot{P}_k$) and the local clearance velocity (U_k) are known. Their determination in this model is described in the following sections.

Equation 12 provides also a condition to test for airway clogging. If the result from the two terms inside the square root is negative, this means that the clearance velocity is too slow to transport the required mucus flow rate through the whole airway cross-section, which would cause the airways to clog. Although airway clogging actually occurs in severe disease states, the present model is not designed to deal with clogging and parameter sets resulting in clogging should be disregarded.

3.3 Distributed mucus production

For the distribution of the mucus production along the conducting airways there are no human data currently available. As an approximation for the distribution of mucus secretion in humans, the airway surface density of total secretory material measured by Plopper et al. (1989) in various lung generations of the rhesus monkey was adopted. The rhesus monkey is considered in many aspects one of the animals closest to humans, and their similarity in terms of airway surface morphology is well established (Jeffery (1983)).

The volume of total secretory product in the surface epithelium and in submucosal glands per unit airway area measured by Plopper et al. (1989) in specific generations of the monkey's lung was as shown in Table 4.

Generation	Total
0	3.671
3	4.179
6	3.086
11	2.169
13	1.039
15	0.656

Table 4. Distribution of total mucus secretory product in rhesus monkey [$\times 10^{-3}$ mm^3/mm^2] (from Plopper et al. (1989)).

By assuming that the total secretory product per unit airway area is proportional to the amount actually produced per unit area, and by assuming these values scale to humans simply with the airway surface area, i.e. the same rates per unit area apply, these distributed rates were transferred and directly applied to the human lung model. To obtain intermediate values for the missing generations, two straight lines were fit to the data. The first curve fit was a simple interpolation between the first two points. For the second curve fit the value at generation 15 was disregarded. Not only is generation 15 beyond the assumed end of the tracheobronchial region, but also its inclusion would cause the resulting curve fit to end too abruptly at generation 14. With the actual, adjusted values shown in Table 5 the resulting curve tends to zero at generation 16, which agrees better with the adopted lung model (see Fig. 4).

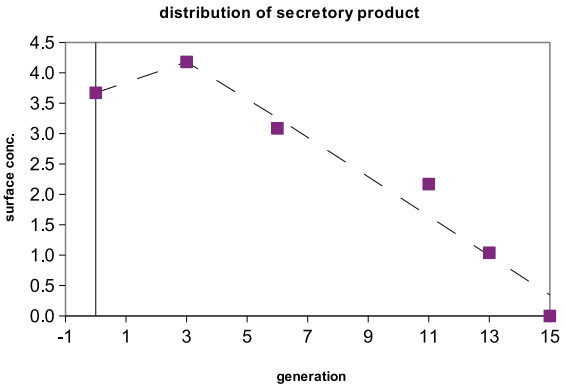

Fig. 4. Distributed mucus production (volumetric surface production [$\times 10^{-3}$ mm^3/mm^2]) and curve fits (eqs. 13 and 14).

Generation	Adjusted Surf. Production
0	3.671
3	4.179
6	3.086
11	2.169
13	1.039
15	0.000

Table 5. Distribution of volumetric mucus production in humans [$\times 10^{-3}$ mm^3/mm^2].

The fitted curves shown in Fig. 4 and used to calculate the distributed local mucus production per unit area $\dot{p}''_k$ correspond to the following functions

$$\text{For generations } 0-3: \qquad \dot{p}''_k = 0.1693\,k + 3.671 \tag{13}$$

$$\text{For generations } 3-14: \qquad \dot{p}''_k = -0.3238\,k + 5.203 \tag{14}$$

where k is the generation and the result is in $\times 10^{-3}$ mm^3/mm^2. Table 6 shows the corresponding values in each generation.

The distributed local mucus production per unit area $\dot{p}''_k$ is combined with the dimensions of the adopted lung geometry model to result in reference values of average mucus production rates in each generation, according to the following equation

$$\dot{p}_{k,\text{ref}} = \dot{p}''_k \left(2^k\,\pi\,L_k\,D_k\right) \tag{15}$$

Equation 15 combined with eq. 9 result in a reference profile of distributed mucus production in the airways, $\dot{P}_{k,\text{ref}}$. Since the production rate of mucus varies from person to person and can also vary with time for the same individual, this reference profile of mucus production is used to scale the actual production profile according to the value of actual total daily production of the subject, $\dot{P}_{\text{tot}}$. A reasonable daily production amount for a healthy, non-smoking adult is 10 ml/day. Typically, a range of values is used in the calculations with 5 ml/day being a reasonable minimum for an adult, and 30 ml/day or greater being considered hypersecretion,

Generation	Surface Production
0	3.67
1	3.84
2	4.01
3	4.18
4	3.91
5	3.58
6	3.26
7	2.94
8	2.61
9	2.29
10	1.97
11	1.64
12	1.32
13	0.99
14	0.67

Table 6. Distribution of volumetric mucus production $\dot{p}_k''$ in humans [$\times 10^{-3}$ mm^3/mm^2].

requiring therapy (Hardy & Anderson (1996)). In fact, patients with severe bronchorrhea have been reported to produce in average more than 60 ml/day (Tamaoki et al. (1994)).

The actual cumulative production values are obtained by modifying the reference values with a scaling factor, namely the ratio between the prescribed total daily production and the cumulative reference production at the trachea (gen. 0)

$$\dot{P}_k = \left(\frac{\dot{P}_{\text{tot}}}{\dot{P}_{0,\text{ref}}} \right) \dot{P}_{k,\text{ref}} \tag{16}$$

Equation 16 provides the actual cumulative production required in eq. 12.

3.4 Mucus clearance velocity

The airway mucus is a highly viscoelastic fluid that is transported by the lung clearance mechanism (cilia beating) from the terminal bronchioli to the trachea. Due to its viscoelasticity, the mucus forms a continuous layer that flows with almost no mixing. Inhaled particles trapped in this layer are transported smoothly and continuously towards the trachea, where they are swallowed. This mucociliary clearance process can be treated as a series of "escalators" that transport mucus and whatever it is carrying from one generation to the next with constant velocity within each generation.

If a tracer substance is inhaled and its clearance measured, the time to clear the trachea (the first generation to be cleared) would be $\tau_0 = L_0/U_0$, where U_0 is the constant mucus transport velocity at the trachea. The amount of tracer deposited in the main bronchi, the next generation to be cleared, would require the time to travel through the bronchi, $\tau_1 = L_1/U_1$, plus the time to travel through the trachea τ_0 to be cleared. This process is illustrated in Fig. 5. In general, measuring from the time when the first particles deposited in generation k begin

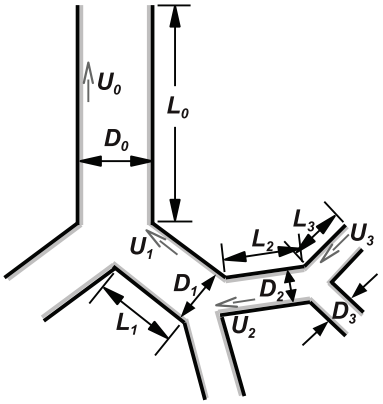

Fig. 5. Schematic of the mucociliary escalator.

to be cleared until the time when the last particles from that generation are cleared results in

$$\sum_{i=0}^{k} \tau_i - \sum_{j=0}^{k-1} \tau_j = \sum_{i=0}^{k} \frac{L_i}{U_i} - \sum_{j=0}^{k-1} \frac{L_j}{U_j} = \frac{L_k}{U_k} = \tau_k \tag{17}$$

By combining cumulative deposition data from the lung deposition model and the *in vivo* clearance data from Stahlhofen et al. (1980) the time τ_k required to clear each generation was determined. Fig. 6 illustrates this process.

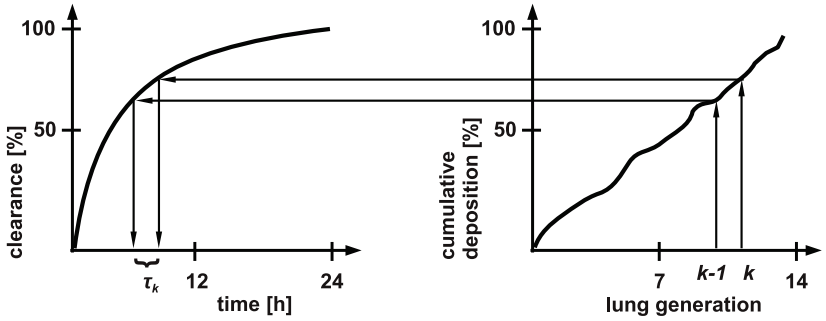

Fig. 6. Time to clear generation k obtained from comparison between cumulative deposition and clearance data.

Four cases measured by Stahlhofen et al. (1980) (breathing pattern A (op. cit., Fig. 8): subject 1 and d_a=9.5 μm, subject 4 and d_a=9.1 μm; breathing pattern B (op. cit., Fig. 9): subject 1 and d_a=7.5 μm, subject 4 and d_a=7.3 μm) were calculated with the 1-D deposition model from Finlay & Stapleton (1995), using the lung geometry dimensions from Finlay (2001). Note that the length of the trachea was shortened by 3 cm, because of the way the tracheobronchial region was imaged in Stahlhofen et al. (1980). The resulting velocity profiles were scaled with a reference clearance velocity at the trachea ($U_{0,\mathrm{ref}} = 5.5$ mm/min) and averaged so that a standard reference clearance velocity profile was generated. This reference profile of

mucus transport velocities in each generation ($U_{k,\mathrm{ref}}$) is shown in Table 7. Figure 7 shows a comparison of the present reference velocity profile with other similar profiles estimated by Lee et al. (1979), Yu et al. (1986) and Cuddihy & Yeh (1988). All profiles were scaled to a tracheal clearance velocity of 5.5 mm/min.

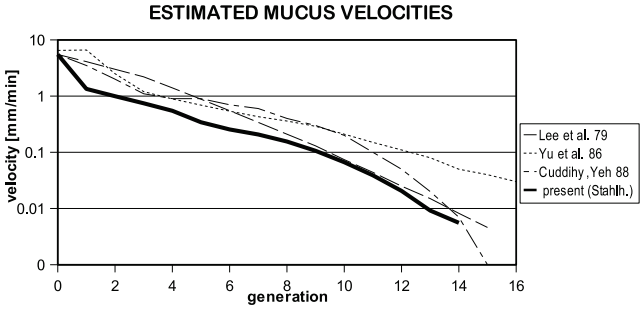

Fig. 7. Comparison of clearance velocity profiles (all profiles scaled to U_0=5.5 mm/min).

Generation	Clearance Velocity
0	5.5000
1	1.3415
2	0.9943
3	0.7439
4	0.5477
5	0.3425
6	0.2551
7	0.2073
8	0.1554
9	0.1063
10	0.0667
11	0.0389
12	0.0206
13	0.0092
14	0.0056

Table 7. Clearance velocity profile ($U_{k,\mathrm{ref}}$ in [mm/min], constant in each generation).

Similarly to the variability in the daily mucus production rate, the clearance velocity also shows variation between individuals and for a single individual, depending on their physical activity, for instance. The linear velocity of mucus flow in the trachea in young nonsmokers has been measured by marker particle clearance as typically 10–15 mm/min (Wanner et al. (1996)). CF patients have been assessed with tracheal clearance velocities that range from essentially zero up to these normal values Yeates et al. (1975).

Here again the actual clearance velocities used in the model are obtained by scaling the entire profile with the ratio between the prescribed tracheal velocity $U_{0,\mathrm{set}}$ and the reference value $U_{0,\mathrm{ref}}$ as follows

$$U_k = \left(\frac{U_{0,\mathrm{set}}}{U_{0,\mathrm{ref}}} \right) U_{k,\mathrm{ref}} \tag{18}$$

Equation 18 provides the actual clearance velocities required in eq. 12.

Using the clearance velocity profiles shown in Fig. 7 and a distributed mucus production based on eqs. 13 and 14, scaled to a total of 10 ml/day, a comparison of estimated mucus layer thicknesses can be calculated. The results are shown in Fig. 8.

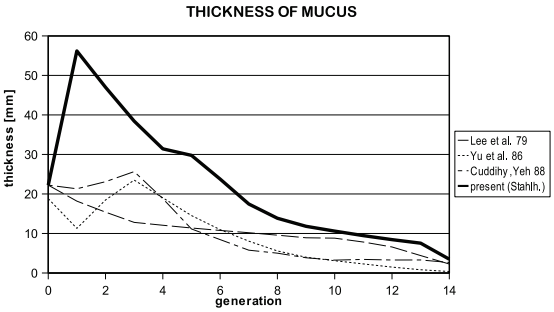

Fig. 8. Comparison of mucus layer thicknesses based on clearance velocities from Fig. 7 and 10 ml/day distributed production.

Combining the thicknesses of the mucus and the PCL layers, the total volume of ASL in each generation can be finally calculated using eq. 2.

4. Modelling local lung concentration of topically active drugs

Once the mass of drug deposited in each generation is obtained with the aerosol deposition model, and the volume of ASL in each generation is obtained with the ASL model, local concentration values can be estimated.

Pharmaceutical aerosols are often an aqueous solution or suspension and the water they carry contributes to the dilution of the drug in the ASL. In addition to knowing the mass of drug deposited in each generation, $m_{k,\text{drug}}$, it is important to also keep track of the mass of water deposited together with the drug, $m_{k,\text{water}}$. If the aerosol is hygroscopic, evaporation may take place in the first few generations and condensation may occur deeper in the more distal airways. The deposition model should account for these changes. We can convert the deposited mass of drug and water to the corresponding volume of deposited aerosol, using

$$V_{k,\text{aerosol}} = \frac{m_{k,\text{drug}}}{\rho_{\text{eff}}} + \frac{m_{k,\text{water}}}{\rho_{\text{water}}} \tag{19}$$

where ρ_{eff} and ρ_{water} are the effective density of the drug formulation and of water, respectively.

All the required information is now available to estimate the average concentration of the drug in the mucus layer, $C_{k,\text{ML}}$, or in the total ASL layer, $C_{k,\text{ASL}}$, in each generation

$$C_{k,\text{ML}} = \frac{m_{k,\text{drug}}}{(V_{k,\text{ML}} + V_{k,\text{aerosol}})} \tag{20}$$

$$C_{k,\text{ASL}} = \frac{m_{k,\text{drug}}}{(V_{k,\text{ASL}} + V_{k,\text{aerosol}})} \tag{21}$$

To account for inter-subject variability and other uncertainties, ranges of physiological values should be used, resulting in minimum and maximum expected concentration values. Table 8 lists a range of physiological values that can be used.

	unit	Min.	Nominal	Max.
Tracheal Clearance Velocity	mm/min	5	10 to 15	20
Daily Mucus Production	ml/day	5	10	60

Table 8. Range of physiological values of input quantities to the model.

The result of the model is a series of concentration curves for each scenario. These local concentrations are then compared with efficacy levels and toxicity levels of the drug, to verify if they are within those limits. The type of delivery device and the prescribed dosage can be adjusted to optimize the predicted concentration levels, thus increasing the likelihood of a successful outcome.

5. Advances in delivery devices

Recent advances of drug delivery devices have increased substantially their efficiency and their ability to adjust the dose delivered to the lung. From the low cost vented jet nebulizers to the more sophisticated breath-actuated, also known as smart nebulizers, the current generation of inhalers allows for the efficient delivery of large doses with an increasing ability to control the amount delivered. Both aspects are important when delivering antibiotics to the lung. Efficient delivery of a large dose may be required to ensure MIC levels are reached. At the same time, control over the dosage is required to ensure that toxicity levels of the antibiotic are not exceeded.

Despite the development of competing types of devices for drug delivery to the lung, from metered dose inhalers to dry powder inhalers, jet nebulizers have never been completely replaced. They are still capable of delivering the largest dosages to the lung. The ability to contain high volume fills makes them uniquely adapted for this purpose. Many types of continuous output nebulizers are on the market today. Among them, valved vented (also called breath enhanced) jet nebulizers reduce the amount of drug lost during exhalation by delivering aerosol preferentially during inhalation. Less affordable, but more compact, ultrasonic nebulizers find widespread use in many clinical settings. Finlay, Stapleton & Zuberbuhler (1998) compared various traditional nebulizers and found a large variation in the predicted lung dosage between the devices.

Nebulizers have experienced a revival through the introduction of so-called “smart nebulizers” (Smaldone (2002)). This is a relatively informal classification that includes all the liquid atomizers, which either use or control the breathing pattern for targeted drug delivery. The technologies used for liquid atomization may vary, but these smart nebulizers have in common the attempt to link aerosol generation with the patient inhalation. Examples of smart nebulizers based on jet nebulization are the breath actuated AeroEclipse® (MMC), the Prodose AAD® System (Profile/Respironics), and the AKITA® system (InAMed). Other smart nebulizers or liquid atomizers use different nebulization technologies. Aerodose® (Aerogen) and eFlow® (Pari) are examples of vibrating orifice based nebulizers, which are capable of more precise dosing. All these new devices incorporate breath actuation and some level of drug delivery control and feedback. Ideally, these monitoring capabilities of the delivered dosage and control of aerosol emission in smart nebulizers could be coupled with

an embedded processing unit that estimates the actual deposited dose in the lung, allowing for individually adjusted treatment with the highest probability of successful outcome, as suggested by Lange & Finlay (2006).

This desirable ability to ensure that a prescribed dosage is effectively delivered to the lung is particularly important in the case of antibiotic treatment of lung infections in cystic fibrosis, to reduce the risk of promoting drug resistance through low concentration levels of antimicrobial in the ASL.

6. Applications of the model

The ASL concentration model described above could be in the future incorporated into the control and feedback systems of smart nebulizers, coaching individual patients to inhale the precise dosage required to reach the MIC as estimated by the model.

Currently, the ASL concentration model can be of vital assistance to the design of clinical trials to increase the chances of a positive outcome by ensuring proper concentration levels are achieved in the lung during the tests. An example of how this model can be used to improve the outcome of clinical trials was described by Hasan & Lange (2007). Two antibiotics were compared, using data from the literature. One of the two was tobramycin, an inhaled antibiotic, which is widely used by CF patients. The other example was taurolidine, which was considered for use against *B. cepacia* in CF patients, but failed to produce results in its first clinical trial with delivery by inhalation.

Using the same input parameters described in Hasan & Lange (2007) for the case of tobramycin, corresponding to the study of Ramsey et al. (1999), the estimates of ASL concentration of the antibiotic were recalculated with increased accuracy by taking into account hygroscopic effects in the aerosol size distribution. The new estimates, shown in Fig. 9, result in slightly increased concentrations, which confirm the prediction that concentration levels well exceeded the value of 0.08 mg/mL, or ten times higher than the *in vitro* MIC value, recommended for *in vivo* efficacy against *P. aeruginosa*. These concentration levels were predicted for all 16 scenarios within the range of input parameters studied, while Fig. 9 only shows a few representative cases, including the maximum and minimum curves of the range.

A different outcome befell a clinical trial of taurolidine, a promising drug candidate against *P. aeruginosa* and *B. cepacia* in CF. The outcome of the randomized double-blinded placebo-controlled crossover trial by Ledson et al. (2002), showed no improvement in sputum *B. cepacia* colony counts. As a consequence of this result, development of the inhaled form of this new drug was halted.

Using model input data that matched as closely as possible the study by Ledson et al. (2002), the above-described model estimated ASL concentration levels that in many cases did not exceed the *in vitro* MIC values of 0.4 mg/mL (see Fig. 10), when it is known that *in vivo* concentrations need to be much higher for successful antimicrobial effect.

The higher end of the predictions reached approximately 5 times the *in vitro* MIC, but this scenario (high mucociliary clearance velocity and low mucus production) corresponds more likely to a non-CF patient, such as the single case reported by Ledson et al. (2000). Taking this higher concentration (2 mg/mL) as a new required level, one could use the ASL concentration model to help design a hypothetical trial that would ensure such levels were reached in the

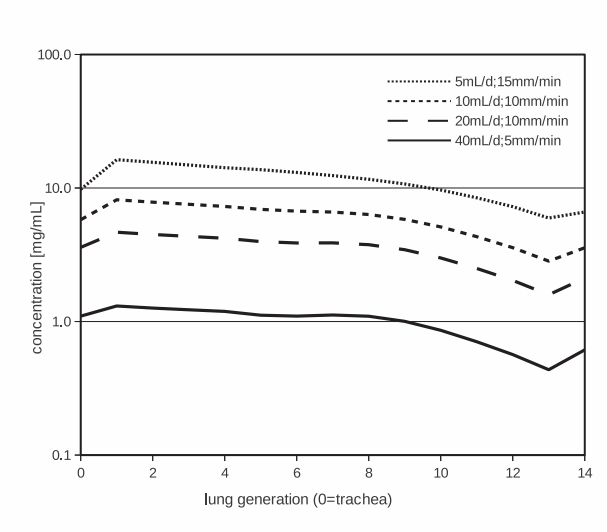

Fig. 9. Estimated ASL concentration of tobramycin in clinical trial.

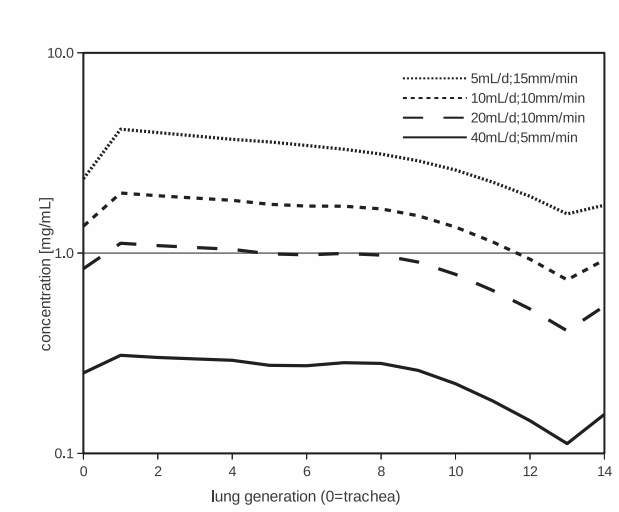

Fig. 10. Estimated ASL concentration of taurolidine in clinical trial.

majority of the cases. Figure 11 demonstrates such a scenario, which could be achieved with a slightly larger nebulizer fill and a significantly larger concentration of taurolidine in the solution.

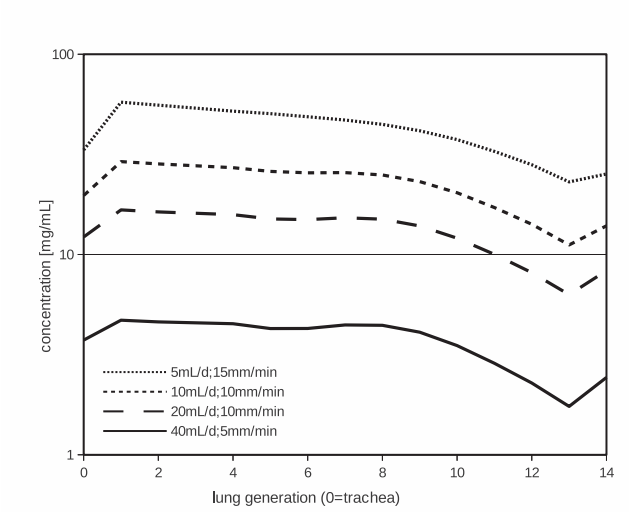

Fig. 11. Estimated ASL concentration of taurolidine in a hypothetical trial that were designed with assistance of the ASL concentration model.

Although a new trial design with higher ASL concentrations would still not be guaranteed to succeed, it would at least stand a better chance of a positive outcome that would allow the continuation of the new drug development.

We conclude that the ASL concentration model is an important tool in the design of clinical trials of inhaled drugs that require a certain concentration level in the lung mucus or the ASL for efficacy.

Similarly, in later stages of the development of a new inhaled drug, the ASL concentration model can greatly assist in the selection of the most appropriate drug delivery device and in establishing the most adequate treatment protocols.

7. Acknowledgements

The mucus and ASL models were developed by the author under the supervision of W. Finlay and in close collaboration with M. King. Their contribution is gratefully acknowledged.

8. References

Böhm, R., Nikodemova, D. & Holy, K. (2003). Use of various microdosimetric models for the prediction of radon induced damage in human lungs, *Radiat. Prot. Dosim.* 104(2): 127–137.

Cuddihy, R. G. & Yeh, H. C. (1988). *Respiratory tract clearance of particles and substances dissociated from particles*, Springer, Berlin, chapter 11, pp. 169–193.

Dailey, H. L. & Ghadiali, S. N. (2007). Fluid-structure analysis of microparticle transport in deformable pulmonary alveoli, *J. Aerosol Sci.* 38: 269–288.

DeHaan, W. H. & Finlay, W. H. (2001). *In vitro* monodisperse aerosol deposition in a mouth and throat with six different inhalation devices, *J. Aerosol Med.* 14(3): 361–367.

DeHaan, W. H. & Finlay, W. H. (2004). Prediciting estrathoracic deposition from dry powder inhalers, *J. Aerosol Sci.* 35(3): 309–331.

Desai, T. R., Tyrrell, G. J., Ng, T. & Finlay, W. H. (2003). In vitro evaluation of nebulization properties, antimicrobial activity and regional airway surface liquid concentration of liposomal polymyxin B sulfate, *Pharm. Res.* 20: 442–447.

Egan, M. J. & Nixon, W. (1985). A model of aerosol deposition in the lung for use in inhalation dose assessments, *Radiation Protection Dosimetry* 11(1): 5–17.

Ferron, G. A., Kreyling, W. G. & Haider, B. (1988). Inhalation of salt aerosol particles – II. Growth and deposition in the respiratory tract, *J. Aerosol Sci.* 19(5): 611–631.

Finlay, W. H. (2001). *The Mechanics of Inhaled Pharmaceutical Aerosols: An Introduction*, Academic Press, London.

Finlay, W. H., Hoskinson, M. & Stapleton, K. W. (1998). Can models be trusted to subdivide lung deposition into alveolar and tracheobronchial fractions?, *Respiratory Drug Delivery VI*, Interpharm Press, Buffalo Grove, IL, USA, pp. 235–242.

Finlay, W. H., Lange, C. F., King, M. & Speert, D. P. (2000). Lung delivery of aerosolized dextran, *Am. J. Respir. Crit. Care Med.* 161: 91–97.

Finlay, W. H., Lange, C. F., Li, W.-I. & Hoskinson, M. (2000). Validating deposition models in disease: what is needed?, *J. Aerosol Med.* 13: 381–385.

Finlay, W. H. & Stapleton, K. W. (1995). The effect on regional lung deposition of coupled heat and mass transfer between hygroscopic droplets and their surrounding phase, *J. Aerosol Sci.* 26(4): 655–670.

Finlay, W. H., Stapleton, K. W. & Zuberbuhler, P. (1997). Predicting regional lung dosages of a nebulized suspension: Pulmicort® (budesonide), *Part. Sci. Technol.* 15: 243–251.

Finlay, W. H., Stapleton, K. W. & Zuberbuhler, P. (1998). Variations in predicted regional lung deposition of salbutamol sulphate between 19 nebulizer models, *J. Aerosol Med.* 11: 65–80.

Forbes, B., Asgharian, B., Dailey, L. A., Ferguson, D., Gerde, P., Gumbleton, M., Gustavsson, L., Hardy, C., Hassall, D., Jones, R., Lock, R., Maas, J., McGovern, T., Pitcairn, G. R., Somers, G. & Wolff, R. K. (2011). Challenges in inhaled product development and opportunities for open innovation, *Adv. Drug Deliv. Rev.* 63: 69–87.

Grgic, B., Finlay, W. H., Burnell, P. K. P. & Heenan, A. F. (2004). *In vitro* intersubject and intrasubject deposition measurements in realistic mouth-throat geometries, *J. Aerosol Sci.* 35(1): 1025–1040.

Hardy, K. A. & Anderson, B. D. (1996). Noninvasive clearance of airway secretions, *Respir. Care Clin. N. Am.* 2: 323–345.

Hasan, M. A. & Lange, C. F. (2007). Estimating *in vivo* airway surface liquid concentration in trials of inhaled antibiotics, *J. Aerosol Med.* 20(3): 282–293.

Heenan, A. F., Finlay, W. H., Grgic, B., Pollard, A. & Burnell, P. K. P. (2004). An investigation of the relationship between the flow field and regional deposition in realistic extra-thoracic airways, *J. Aerosol Sci.* 35: 1013–1023.

James, A. C., Stahlhofen, W., Rudolf, G., Egan, M. J., Nixon, W., Gehr, P. & Briant, J. K. (1991). The respiratory tract deposition model proposed by the ICRP task group, *Radiation Protection Dosimetry* 38(1): 159–165.

Jeffery, P. K. (1983). Morphologic features of airway surface epithelial cells and glands, *Am. Rev. Respir. Dis.* 128: S14–S20.

Kimmel, E. C., Reboulet, J. E. & Carpenter, R. L. (2001). A typical path model of tracheobronchial clearance of inhaled particles in rats, *Toxicol. Ind. Health* 17: 277–284.

Lange, C. F. & Finlay, W. H. (2006). Liquid atomising: nebulizing and other methods of producing aerosols, *J. Aerosol Med.* 19(1): 28–35.

Lange, C. F., Hancock, R. E. W., Samuel, J. & Finlay, W. H. (2001). *In vitro* aerosol delivery and regional airway surface liquid concentration of a liposomal cationic peptide, *J. Pharm. Sci.* 90(10): 1647–1657.

Ledson, M. J., Cowperthwaite, C., Walshaw, M. J., Gallagher, M. J., Williets, T. & Hart, C. A. (2000). Nebulized taurolidine and *B. cepacia* bronchiectasis, *Thorax* 55: 91–93.

Ledson, M. J., Gallagher, M. J., Robinson, M., Cowperthwaite, C., Williets, T., Hart, C. A. & Walshaw, M. J. (2002). A randomized double-blinded placebo-controlled crossover trial of nebulized taurolidine in adult cystic fibrosis patients infected with *Burkholderia cepacia*, *J. Aerosol Med.* 15(1): 51–57.

Lee, P. S., Gerrity, T. R., Hass, F. J. & Lourenco, R. V. (1979). A model for tracheobronchial clearance of inhaled particles in man and a comparison with data, *IEEE Trans. Biomed. Eng.* BME-26(11): 624–629.

Martonen, T. B., Yang, Y. & Hwang, D. (1994). Hygroscopic behaviour of secondary cigarette smoke in human nasal passages, *S.T.P. Pharma Sciences* 4: 69–76.

Matsui, H., Randell, S. H., Peretti, S. W., Davis, C. W. & Boucher, R. C. (1998). Coordinated clearance of periciliary liquid and mucus from airway surfaces, *J. Clin. Invest.* 102(6): 1125–1131.

Mitsakou, C., Helmis, C. & Housiadas, C. (2005). Eulerian modelling of lung deposition with sectional representation of aerosol dynamics, *J. Aerosol Sci.* 36: 75–94.

Plopper, C. G., Heidsiek, J. G., Weir, A. J., St. George, J. A. & Hyde, D. M. (1989). Tracheobronchial epithelium in the adult rhesus monkey: a quantitative histochemical and ultrastructural study, *Am. J. Anat.* 184: 31–40.

Ramsey, B. W., Pepe, M. S., Quan, J. M., Otto, K. L., Montgomery, A. B., Warren, J. W., Vasilijev, K. M., Borowitz, D., Bowman, C. M., Marshall, B. C., Marshall, S. & Smith, A. L. (1999). Intermittent administration of inhaled tobramycin in patients with cystic fibrosis, *New Eng. J. Med.* 340(1): 23–30.

Roth, A. P., Lange, C. F. & Finlay, W. H. (2003). The effect of breathing pattern on nebulizer drug delivery, *J. Aerosol Med.* 16(3): 325–339.

Serafini, S. M. & Michaelson, E. D. (1977). Length and distribution of cilia in human and canine airways, *Bull. Europ. Physiopath. Resp.* 13: 551–559.

Smaldone, G. C. (2002). Smart nebulizers, *Respir. Care* 47: 1434–1441.

Stahlhofen, W., Gebhart, J. & Heyder, J. (1980). Experimental determination of the regional deposition of aerosol particles in the human respiratory tract, *Am. Ind. Hyg. Assoc. J.* 41(6): 385–398a.

Stahlhofen, W., Gebhart, J., Heyder, J. & Scheuch, G. (1983). New regional deposition data of the human respiratory tract, *J. Aerosol Sci.* 14: 186–188.

Sweeney, L. G., Wang, Z., Loebenberg, R., Wong, J. P., Lange, C. F. & Finlay, W. H. (2005). Spray-freeze-dried liposomal ciprofloxacin powder for inhaled aerosol drug delivery, *Int. J. Pharm.* 305: 180–185.

Tamaoki, J., Chiyotani, A., Tagaya, E., Sakai, N. & Konno, K. (1994). Effect of long term treatment with oxitropium bromide on airway secretion in chronic brochitis and diffuse panbronchiolitis, *Thorax* 49: 545–548.

Taulbee, D. B. & Yu, C. P. (1975). A theory of aerosol deposition in the human respiratory tract, *J. Appl. Physiol.* 38(1): 77–85.

Wang, Z., Cheng, H. T., Roa, W. & Finlay, W. H. (2003). Farnesol for aerosol inhalation: nebulization and activity against human lung cancer cells, *J. Pharm. Sci.* 6: 95–100.

Wanner, A., Salathé, M. & O'Riordan, T. G. (1996). Mucociliary clearance in the airways, *Am. J. Respir. Crit. Care Med.* 154: 1868–1902.

Weibel, E. R. (1963). *Morphology of the human lung*, Acedemic Publishers, New York.

Widdicombe, J. G. (1997). Airway surface liquid: concepts and measurements, *in* D. F. Rogers & M. I. Lethem (eds), *Airway Mucus: Basic Mechanisms and Clinical Perspectives*, Birkhäuser, Basel, chapter 1, pp. 1–17.

Yeates, D. B., Sturgess, J. M., Kahi, S. R., Levison, H. & Aspin, N. (1975). Mucociliary transport in trachea of patients with cystic fibrosis, *Arch. Dis. Childhood* 51: 28–33.

Yu, C. P., Hu, J. P., Yen, B. M., Spektor, D. M. & Lippmann, M. (1986). *Models for mucociliary particle clearance in lung airways*, Lewis, Chelsea, Michigan, chapter 39, pp. 569–578.

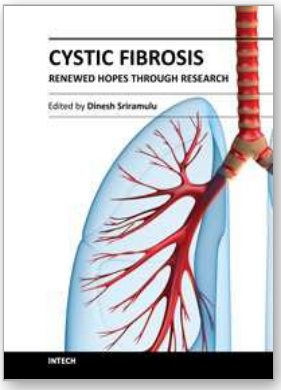

Cystic Fibrosis - Renewed Hopes Through Research

Edited by Dr. Dinesh Sriramulu

ISBN 978-953-51-0287-8
Hard cover, 550 pages
Publisher InTech
Published online 28, March, 2012
Published in print edition March, 2012

Living healthy is all one wants, but the genetics behind creation of every human is different. As a curse or human agony, some are born with congenital defects in their menu of the genome. Just one has to live with that! The complexity of cystic fibrosis condition, which is rather a slow-killer, affects various organ systems of the human body complicating further with secondary infections. That's what makes the disease so puzzling for which scientists around the world are trying to understand better and to find a cure. Though they narrowed down to a single target gene, the tentacles of the disease reach many unknown corners of the human body. Decades of scientific research in the field of chronic illnesses like this one surely increased the level of life expectancy. This book is the compilation of interesting chapters contributed by eminent interdisciplinary scientists around the world trying to make the life of cystic fibrosis patients better.

How to reference

In order to correctly reference this scholarly work, feel free to copy and paste the following:

Carlos F. Lange (2012). Improving the Likelihood of Success in Trials and the Efficiency of Delivery of Mucolytics and Antibiotics, Cystic Fibrosis - Renewed Hopes Through Research, Dr. Dinesh Sriramulu (Ed.), ISBN: 978-953-51-0287-8, InTech, Available from: http://www.intechopen.com/books/cystic-fibrosis-renewed-hopes-through-research/improving-the-likelihood-of-success-in-trials-and-efficiency-of-delivery-of-mucolytics-and-antibioti

INTECH
open science | open minds

InTech Europe
University Campus STeP Ri
Slavka Krautzeka 83/A
51000 Rijeka, Croatia
Phone: +385 (51) 770 447
Fax: +385 (51) 686 166
www.intechopen.com

InTech China
Unit 405, Office Block, Hotel Equatorial Shanghai
No.65, Yan An Road (West), Shanghai, 200040, China
中国上海市延安西路65号上海国际贵都大饭店办公楼405单元
Phone: +86-21-62489820
Fax: +86-21-62489821